Discrepancies between Theory and Experiment in Determining the Ionization Energy of NF_3

Megan R. Bentley,[*,†] Peter R. Franke,[†] Kaila E. Weflen,[†] David H. Bross,[‡] Branko Ruscic,[*,‡] and John F. Stanton[†,¶]

†*Quantum Theory Project, Department of Chemistry, University of Florida, Gainesville, FL 32611, USA.*

‡*Chemical Sciences and Engineering Division, Argonne National Laboratory, Lemont, IL 60439, USA.*

¶*Deceased March 21, 2025*

E-mail: mgbentley@ufl.edu; ruscic@anl.gov

Abstract

High-accuracy *ab initio* thermochemical predictions for the ionization energy of NF_3, the barrier height (to inversion) of NF_3^+, and the dissociative ionization threshold of NF_3 to NF_2^+ + F are presented and incorporated into Active Thermochemical Tables. The adiabatic ionization energy of the first ionization band of NF_3, calculated at 12.647 ± 0.010 eV, is at odds with previous experimental interpretations by nearly 0.36 eV due to unfavorable Franck-Condon factors associated with this transition. The barrier (to inversion) height is calculated to be about 0.6 eV lower in energy than the prior interpretation, which instigates a discussion of supposed vibrational structure of the first ionization band of NF_3. Updated assignments of the photoelectron spectrum are

proposed, and the loss in vibrational spacing on the high energy side of the experimental ionization band is discussed. Rudimentary anharmonic Franck-Condon simulations qualitatively reproduce the broad spectral features observed in experiment.

Introduction

When a molecule undergoes a significant change in geometry upon ionization, it becomes notoriously difficult and often impossible to measure a precise ionization threshold experimentally. One such example is the ionization of the CF_3 radical,[1–6] where the adiabatic ionization energy is 9.068 ± 0.004 eV,[7,8] nearly 2 eV lower in energy than the vertical ionization energy (11.02 eV, as determined by Dossman et al.[6]). Removal of the single unpaired electron on the carbon atom of trigonal pyramidal (C_{3v}) CF_3 renders the corresponding CF_3^+ cation fully planar (D_{3h}), resulting in a photoelectron spectrum characterized by an extensive vibrational progression. Because there are several accessible transitions within the broad envelope, near-threshold transitions possess vastly smaller intensities than those towards the center of the progression, and by comparison, are effectively impossible to discern from the background signal. A calculated Franck-Condon envelope[1] shows that the vertical transition for the ionization of CF_3 occurs near $\nu_2^+ = 20$ in the umbrella mode. However, the lower-energy $\nu_2^+ = 8$ transition intensity is already below 1% of $\nu_2^+ = 20$,[2] and the determination of the true threshold ($\nu^+ = 0$) by photoionization/photoelectron spectroscopic techniques is virtually impossible. Both direct and indirect techniques in the literature[2] face significant challenges when attempting to report an accurate adiabatic ionization energy for this species.

NF_3 (nitrogen trifluoride) is a potent greenhouse gas, second only to SF_6.[9,10] It is industrially used in production of microelectronics, LCD screens, etc. Though NF_3 is stable and commercially available, the experimental determination of its adiabatic ionization energy is plagued by challenges similar to those encountered for CF_3. The loss of an electron from the lone pair on the nitrogen atom[11] again results in substantial flattening of the

trigonal pyramidal structure of the radical ion as compared to that of the neutral. While the NF_3^+ cation maintains C_{3v} symmetry, a rough inspection of its photoelectron spectrum recorded by Berkowitz and Greene[12] shows a broad envelope that spans over two eV with no clearly distinguishable adiabatic ionization threshold. Photoionization spectrometry measurements[13,14] and He I photoelectron studies[12,15–17] estimate the adiabatic ionization threshold to be near 13.0 eV. Coincidence measurements[18] and joint photoelectron spectroscopy (PES)/photoionization mass spectrometry (PIMS) studies[19] produce similar results.

By contrast, mid-level theoretical studies[20,21] using CBS-extrapolated CCSD(T)[22–24] electronic energies predict the ionization threshold to be at least 0.36 eV lower in energy, near 12.6 eV (see Table 1). It is therefore of interest to more closely examine the ionization threshold of NF_3 *via* more accurate theoretical means, in an attempt to address the large discrepancy between experimental and theoretical results in the literature.

It has long been acknowledged that well-established experimental energy differences serve as anchor points for theoretical method development.[4,25] However, when the determination of reliable ionization energies, bond dissociation energies, or enthalpies of formation *via* experimental means is precluded (as in the present case), one is heavily reliant upon theoretical techniques to provide accurate estimates of desired quantities. Many such techniques exist to estimate the full-CI energy at the complete basis set (CBS) limit. These include 'fixed-recipe' protocols such as the closely-related HEAT[26–31] and Wn methods,[32–36] ANL-n schemes,[37] and more flexible model chemistries like focal point analyses (FPA) by Allen and colleagues,[38–40] and Feller-Peterson-Dixon (FPD)[41] techniques. Although these methods execute different theoretical choices in practice, the overarching strategy is the same: the total energy comprises a number of additive contributions that are each computed with some level of theory and a set of bases. Then, subsequent extrapolations and approximations are performed to produce refined estimates of various terms. These techniques have met with much success in the accurate (often within 1 kJ/mol) determination of bond dissociation energies and enthalpies of formation for many small species, operating sometimes nearly

independently from any empirical influence.

One entity that profits directly from the interplay between theory and experiment in this way are the Active Thermochemical Tables (ATcT).[7,8] Using the Thermochemical Network (TN) approach, ATcT extracts accurate thermochemical properties in a manner that is internally consistent with the available experimental and theoretical determinations. In cases when sufficiently high quality experimental data is not available, the bulk of the statistical contribution to predicted thermochemical quantities for certain species can be obtained from purely theoretical determinations.[31] In particular, the most currently publicly available version of ATcT results as of this writing[42] reports IE(NF_3) = 12.636 ± 0.023 eV (*vide infra*), driven primarily by mid-level theoretical predictions (all computed in-house as part of the standard routine of adding a new species to the ATcT TN: (G3X[43] (12.656 eV), G4[44] (12.597 eV), CBS-QB3 (12.647 eV) and CBS-APNO (12.542 eV),[45–47] W1[32] (12.644 eV)), and the aforementioned CBS-extrapolated CCSD(T) determinations.[20,21]

In this study, the high-accuracy extrapolated *ab initio* thermochemistry protocol (HEAT) is used to calculate ionization and fragmentation thresholds for NF_3^+ and NF_2^+ to within 0.01 eV (∼ 1 kJ/mol), with the intent to scrutinize previous theoretical determinations. Moreover, the NF_3^+ barrier to inversion is compared with a value previously postulated,[12] which calls into question the interpretation of the partially resolved vibrational structure in the photoelectron spectrum. Rudimentary anharmonic Franck-Condon simulations are performed to qualitatively validate theoretical predictions of the ionization threshold and discuss any hypothetical 'loss' of vibrational structure on the high-energy side of the broad spectral envelope.

Computational Details

High-Accuracy Extrapolated *ab initio* Thermochemistry (HEAT)

HEAT, as a high-accuracy composite method, has been detailed extensively elsewhere in the literature[26–28,30,31] but is nonetheless briefly summarized here and in Table 2. It centers on an additive approximation where total energies are calculated as the sum of eight individual contributions, as shown below. From these, total atomization energies, barriers to inversion, and appearance thresholds may be determined.

$$\begin{aligned} E &= E^{\infty}_{\mathrm{HF}} + \Delta E^{\infty}_{\mathrm{CCSD(T)}} + \Delta E^{\infty}_{\mathrm{CCSDT}} + \Delta E_{\mathrm{HLC}} \\ &+ \Delta E_{\mathrm{ZPE}} + \Delta E_{\mathrm{REL}} + \Delta E_{\mathrm{SO}} + \Delta E_{\mathrm{DBOC}} \end{aligned} \quad (1)$$

The first four terms comprise the contribution to the non-relativistic electronic energy (Details pertaining to how the first three terms are calculated are located in Refs.[26–28]). The non-relativistic electronic energy is then corrected for zero-point vibrational effects (ΔE_{ZPE}), relativistic (ΔE_{REL}), spin-orbit (ΔE_{SO}), and nuclear kinetic energy effects (ΔE_{DBOC}). Higher-order (beyond CCSDT[48–50]) electron correlation effects (term 4, ΔE_{HLC}), are treated *via* 'perturbative' approximations (CCSDT(Q)[51,52] and CCSDT(Q)$_{\Lambda}$[53–55] or a fully iterative treatment (CCSDTQ[54,56–58]) using a Dunning correlation-consistent, double-zeta (cc-pVDZ) basis set.[59,60] Recently, the overestimation of quadruples contributions provided by CCSDT(Q) has become a nonnegligible focal point for pathological molecules possessing significant multireference character, like ozone, where CCSDT(Q)$_{\Lambda}$ is instead chosen to more faithfully represent the contribution of quadruple excitations to the correlation energy.[61] Extended HEAT studies[30,31] and composite predictions of equilibrium structures and frequencies[62] have also advocated for use of Λ-based perturbative approximations, and such corrections are compared with CCSDT(Q) and fully iterative CCSDTQ in this study.

Auxiliary corrections (zero-point vibration, relativistic, spin-orbit, and nuclear kinetic energy) to the nonrelativistic electronic energy follow exactly the same prescription that can be found in previous HEAT documentation. As is conventional within the HEAT protocol, all single-point calculations are done at the appropriate equilibrium geometry (all electron (ae)-CCSD(T)/cc-pVQZ) for the desired species of interest. Closed-shell species are calculated with a restricted reference wavefunction (RHF) while open-shell species use a fully unrestricted reference (UHF). Expectation values of S^2 did not deviate far from the ideal value of 0.75; the maximum seen was 0.78. All calculations are performed using the CFOUR quantum chemistry program package,[63–67] with the exception of open-shell CCSDT(Q), CCSDT(Q)$_\Lambda$, and CCSDTQ calculations, which use MRCC[68] as interfaced with CFOUR. All calculations included in this work are converged to at minimum the seventh decimal place in energy.

Franck-Condon Simulation

Simulation of the lowest ionized state of NF_3's photoelectron spectrum ($\tilde{X}^+\ ^2A_1 \leftarrow \tilde{X}\ ^1A_1$) at 0 K is based on quartic force fields. The $\tilde{X}\ ^1A_1$ potential energy surface, to fourth-order, is calculated with frozen-core (fc)-CCSD(T)/ANO1 in the (dimensionless) normal coordinates representation referenced at the neutral equilibrium geometry determined with the same level of theory and basis set. The $\tilde{X}^+\ ^2A_1$ surface uses the normal coordinates representation as defined by the $\tilde{X}\ ^1A_1$ electronic state with force constants also calculated with fc-CCSD(T)/ANO1. Only the two symmetric modes are present in the quartic expansions, and the force constants used to describe these surfaces are listed in Table 5. The XSIM program within CFOUR[63,69] uses Lanczos recursion[70] to generate vibrational energy levels using direct product harmonic oscillator basis sets, which are then used to simulate the anharmonic Franck-Condon spectrum displayed in Figure 2.

NF_3^+ Electronic States

The vertical ionization energies (VIEs) of four electronic states of NF_3^+ are calculated at the frozen-core EOMIP-CCSD(T)(a)*[71,72] level of theory with an aug-cc-pVTZ basis set using the closed-shell neutral NF_3 ($\tilde{X}\ ^1A_1$) as the reference state. The neutral's geometry is optimized at the fc-CCSD/aug-cc-pVDZ level of theory. These values are located in Table 4.

Active Thermochemical Tables

The ATcT approach has been described in more detail previously.[7,8] Tersely, as opposed to the sequential approach of developing thermochemistry (A begets B, B begets C, used by virtually all traditional tabulations of enthalpies of formation), the ATcT approach is based on constructing, statistically analyzing, and solving a Thermochemical Network (TN), which contains all available high-quality thermochemical determinations involving the targeted chemical species, such as reaction enthalpies and/or free energies, adiabatic ionization energies, electron affinities, dissociative ionization onsets, etc., both from experiments and theory. The statistical analysis that precedes the final simultaneous solution for all included chemical species identifies potential outliers, i.e. determinations that within their initially assigned (a.k.a. 'prior') uncertainties are inconsistent with the remaining knowledge content of the TN. This, *inter alia*, enables ATcT to successfully arbitrate between apparently conflicting thermochemical determinations based on the prevailing knowledge content of the TN.[31,73–77] With respect to ATcT, the starting point in the present work is the most recent publicly available version of ATcT results.[42,76] The provenance of the corresponding values for the adiabatic ionization energy of NF_3 and the dissociative ionization onset to form the NF_2^+ fragment are analyzed and compared to the HEAT results. Subsequently, a new version of ATcT results is created by adding the calculated HEAT results to the TN, with the aim of further refining the ATcT values for these two quantities.

Results and Discussion

Table 1: Previous literature threshold estimates with accompanying uncertainties. Column 1 lists the first ionization energy of NF_3 (adia. IE (NF_3)) reported by references located in column 2. The third column lists the appearance energy of NF_2^+ from fragmentation of NF_3^+ ($AE_0(NF_2^+/NF_3)$), with appropriate references in column 4.

adia. IE (NF_3)	Ref.	$AE_0(NF_2^+/NF_3)$	Ref.
Experiment			
13.00 ± 0.02	[13]	14.12 ± 0.01	[13,78]
13.00 ± 0.10	[15,16]	14.100 ± 0.008	[14]
12.97 ± 0.04	[17]	14.11 ± 0.10	[11]
13.00 ± 0.05	[12]		
13.06 ± 0.20	[19]		
12.94 ± 0.01	[18]		
Theory			
12.64 ± 0.08	[20]		
12.639 ± 0.055	[21]		
ATcT[1] (previous)			
12.636 ± 0.023	[42]	14.105 ± 0.007	[42]
HEAT (this work)			
12.647 ± 0.010		14.112 ± 0.010	
ATcT (this work)			
12.644 ± 0.007		14.108 ± 0.005	

Table 2 documents electronic energy contributions (in cm^{-1}) for the adiabatic (column 3) and vertical (column 4) ionization energies of NF_3, NF_3^+ inversion barrier height (column 5) and NF_2^+ fragment appearance energy (column 6). Additive terms listed in Equation 1 are listed with more detailed calculation specifications (column 1) and corresponding basis sets (column 2). Terms within braces { } indicate basis-set extrapolated[79,80] values. Rows bolded and marked with asterisks indicate which calculations are included in the final HEAT determinations of the desired thermochemical quantity.

Convergence toward the CBS limit for the nonrelativistic energetic contributions is straightforward to track and compare with extrapolated results. It can also be seen that CCSDT(Q)$_\Lambda$ is closer to the CCSDTQ ΔE_{HLC} contribution than CCSDT(Q) in all cases, affirming the

Table 2: Contributions to electronic energy differences (in cm^{-1}). adia. IE and vert. IE indicate adiabatic and vertical ionization energies of NF_3. $\Delta^{\ddagger} NF_3^+$ corresponds to the barrier to inversion height of the NF_3^+ cation, and $AE_0(NF_2^+/NF_3)$ the appearance energy for the NF_2^+ fragment.
* Boldfaced rows with asterisks indicate which terms are included in the final sum to produce HEAT(456Q) values for each respective quantity.

Component	Calculation	adia. IE (NF_3)	vert. IE (NF_3)	$\Delta^{\ddagger} NF_3^+$	$AE_0(NF_2^+/NF_3)$
E^{∞}_{SCF}	aCVTZ	91426	105812	3470	97328
	aCVQZ	91139	105696	3456	97056
	aCV5Z	91109	105680	3457	97006
	aCV6Z	91108	105680	3456	97002
	aCV{T,Q,5}Z	91119	105680	3459	96997
	***aCV{Q,5,6}Z**	**91108**	**105680**	**3455**	**97001**
$\Delta E^{\infty}_{ae\text{-}CCSD(T)}$	aCVTZ	9939	4227	889	16338
	aCVQZ	10354	4921	855	17254
	aCV5Z	10495	5142	857	17527
	aCV6Z	10555	5238	857	17646
	aCV{Q,5}Z	10642	5373	859	17814
	***aCV{5,6}Z**	**10638**	**5372**	**857**	**17810**
$\Delta E_{fc\text{-}CCSDT - fc\text{-}CCSD(T)}$	pVTZ	-102	-251	8	-117
	pVQZ	-110	-250	7	-130
	***pV{T,Q}Z**	**-115**	**-250**	**5**	**-139**
ΔE_{HLC}	fc-CCSDT(Q) / pVDZ	1	-227	19	0
	fc-CCSDT$(Q)_{\Lambda}$ / pVDZ	18	-158	12	41
	***fc-CCSDTQ / pVDZ**	**14**	**-156**	**9**	**31**
ΔE_{ZPE}	***ae-CCSD(T) / pVQZ**	**362**		**-297**	**-654**
$\Delta E_{REL\text{-}MVD2}$	***ae-CCSD(T) / aCVTZ**	**2**	**8**	**103**	**-102**
ΔE_{SO}	***Experiment**	**0**	**0**	**0**	**-135**
ΔE_{DBOC}	***SCF / apVTZ**	**-1**	**9**	**4**	**8**
HEAT (cm^{-1})		102009	110663	4137	113820
HEAT (eV)		12.647	13.720	0.513	14.112

Table 3: Comparison of HEAT total atomization energies and CCSD(T) / CBS extrapolated values determined by Grant et al.[21] DBOC corrections are not included in the previous literature scheme and are thus left blank.

	TAE (NF_3)			TAE (NF_3^+)			TAE (NF_2^+)		
Component	Ref.[21]	HEAT	Δ	Ref.[21]	HEAT	Δ	Ref.[21]	HEAT	Δ
$E_{CBS} + \Delta E_{CV}$	71918	72132	214	-29642	-29514	128	-42751	-42572	179
ΔE_{ZPE}	-2291	-2302	-11	-2613	-2664	-51	-1626	-1648	-21
ΔE_{REL}	-234	-130	104	-297	-132	165	-143	-28	116
ΔE_{SO}	-409	-404	5	-409	-404	5	-273	-270	3
ΔE_{DBOC}		11	11		12	12		3	3
Total (cm^{-1})	68983	69306	323	-32961	-32703	259	-44794	-44514	280
Total (kJ/mol)	825.22	829.09	3.86	-394.31	-391.21	3.10	-535.85	-532.50	3.35

Table 4: Vertical ionization energies (VIEs) (in eV) of the four lowest-lying electronic states of NF_3^+, as calculated with fc-EOMIP-CCSD(T)(a)*[72] using an aug-cc-pVTZ basis.

	Electronic State	Expt.[11,17] (eV)	Calculated (eV)
NF_3^+	^2E	17.16	17.40
	^2E	16.15	16.18
	$^2A_2$	16.55	15.82
	$\tilde{X}^+\,^2A_1$	13.73	13.64
NF_3	$\tilde{X}\,^1A_1$	0.0	0.0

Table 5: Force constants (in cm^{-1}) with respect to the neutral electronic state normal coordinates for NF_3, NF_3^+ determined with fc-CCSD(T)/ANO1.

	$\tilde{X}\,^1A_1$ (cm^{-1})	$\tilde{X}^+\,^2A_1$ (cm^{-1})
Δ	0	110663
F_1	0	3428
F_2	0	976
F_{11}	1053	573
F_{12}	0	-13
F_{22}	656	779
ϕ_{111}	-133	-132
ϕ_{112}	65	44
ϕ_{122}	-36	-52
ϕ_{222}	100	102
ϕ_{1111}	-12	1
ϕ_{1112}	-23	-15
ϕ_{1122}	4	5
ϕ_{1222}	-6	-7
ϕ_{2222}	11	11

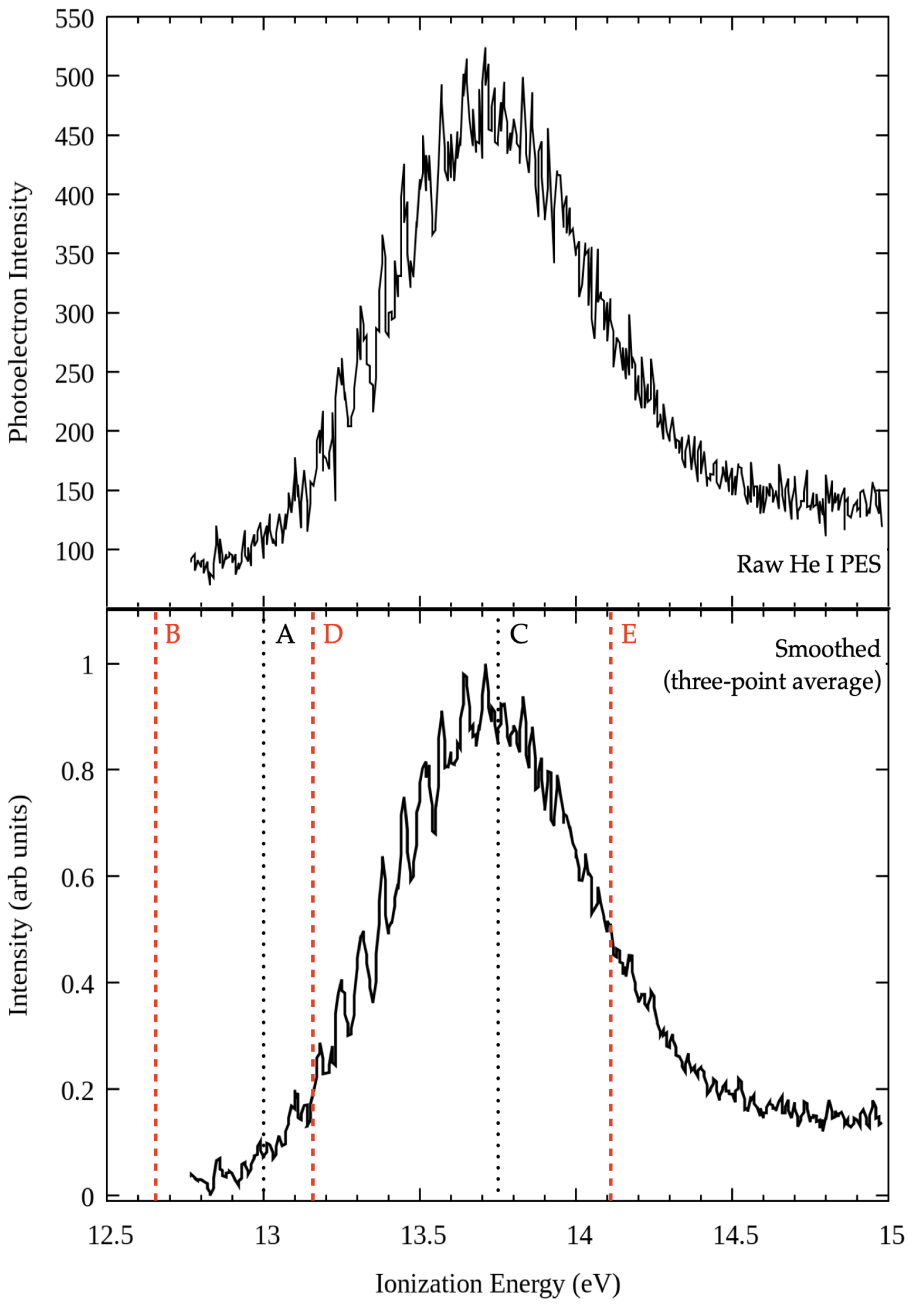

Figure 1: The upper panel displays the raw He I photoelectron spectrum, analogous to upper panel of Fig. 2 in Ref.,[12] reproduced with permission from J. P. Greene, Ref.[12] Copyright 1984, AIP Publishing. The lower panel displays the corresponding spectrum smoothed by a three-point average and annotated by a number of vertical lines. Lines A and C (black, dotted) denote the approximate positions of the adiabatic ionization energy and the peak maximum (and NF_3^+ barrier to inversion), respectively, as reported by Berkowitz and Greene.[12] Lines B, D, and E (red, dashed) mark HEAT-calculated quantities for the NF_3 ionization threshold (B), NF_3^+ barrier to inversion (D), and appearance threshold of NF_2^+ from NF_3 (E) (Table 2).

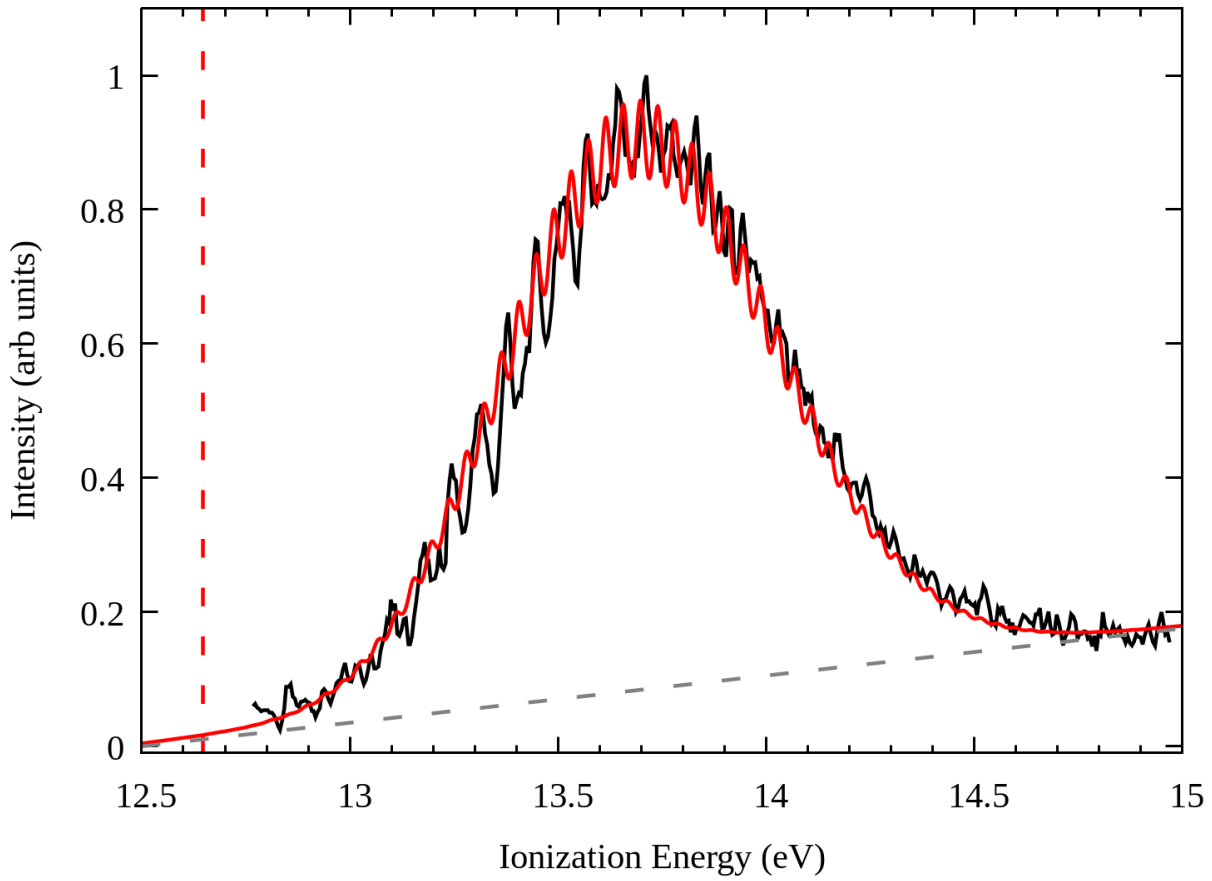

Figure 2: Experimental spectrum,analogous to upper panel of Fig. 2 in Ref.,[12] reproduced with permission from J. P. Greene, Ref.,[12] Copyright 1984, AIP Publishing, smoothed by a three-point average (black), overlaid by qualitative anharmonic Franck-Condon simulation (red). The vertical red dashed line marks the HEAT-calculated IE(NF_3), and the gray dashed line is a simple linear sloping background correction.

aforementioned recommendations for the use of lambda-based methods when prohibited from a fully iterative treatment of quadruple excitations. In the context of this work, CCSDTQ calculations with a cc-pVDZ basis are achievable and are thus used in the final HEAT determination. The vertical ionization energy is not a particularly well defined experimental quantity and is definitely not a thermodynamically consequential quantity. Experimentally, it is typically defined as the maximum in the Franck-Condon envelope, the position of which differs slightly depending on whether the corresponding vibrational progression is clearly resolved or not. For the purpose of an approximate comparison to the experimental spectrum of Berkowitz and Greene,[12] the vertical ionization energy of NF_3^+ is computed here as the difference between the electronic energies of NF_3 and NF_3^+ at the equilibrium geometry of NF_3 (i.e. without a zero-point correction).

While earlier classifications of HEAT[27,28] have advocated for the use of an acronym-based naming scheme to distinguish between various 'flavors' of the method, this practice is abandoned here, partially due to ongoing developments of extended HEAT methods in recent years, as well as to avoid superfluous determinations that vary at maximum by 32 cm^{-1} for the quantities in Table 2, well within the accepted error bars of $\sim$ 1 kJ/mol. However, it is perhaps useful to mention that the final sums in Table 2 are equivalent to a HEAT456-Q determination for each quantity. Non-asterisked contributions found in the table may be used to construct other flavors outlined in previous works.

The ionization energy of NF_3, as determined by HEAT (456-Q), is 12.647 ± 0.010 eV. This is consistent with prior theoretical determinations based on a CBS-extrapolated CCSD(T) scheme[21] and will be elaborated upon in the following section. It is noteworthy that the higher-level correlation contribution to the vertical ionization energy is significantly larger in magnitude than the corresponding value for the adiabatic ionization energy. This can be rationalized by the fact that the energies of NF_3^+ are evaluated at the equilibrium geometry of the *neutral* rather than the NF_3^+ optimized structure, and requires the inclusion of higher-order coupled cluster excitations to be adequately described. Interestingly, however, the

barrier (to inversion) height predicted by HEAT in the NF_3^+ cation is roughly 0.24 eV lower than that rationalized by Berkowitz and Greene,[12] and will be the subject of discussion in the Results and Discussion section labeled 'Interpretation of Experimental Results' .

Comparison with CBS-Extrapolated CCSD(T)

When comparing the HEAT ionization threshold in Table 2 with prior calculations in the literature (Table 1), the adiabatic ionization energies are within 0.008 eV (roughly 65 cm^{-1}) of one another. This is not totally unexpected, as energy differences in thermochemistry are rather robustly determined, even with much less converged levels of theory and basis sets with respect to full CI and CBS limits. Total atomization energies and enthalpies of formation, conversely, are much more difficult to determine accurately. A comparison of total atomization energies calculated *via* the present HEAT method and the prior CBS-extrapolated CCSD(T) scheme in reference[21] has been constructed in Table 3. It is important to point out that the 'HEAT' TAE contributions for the cations listed in this table slightly differ from those tabulated in Table 2 and SI Table 2. In HEAT, the cation total atomization energies are determined *via* $NF_n^+ \rightarrow N^+ + n\,F$, whereas in Table 3, by $NF_n^+ \rightarrow N + n\,F$ to maintain consistency with the method used in.[21] Table 2 in the Supporting Information also contains the relevant atomic information for N, N^+, and F to construct the total atomization energies in either format.

The TAE predictions between the current study and Grant et al.[21] differ by as much as 3.86 kJ/mol (323 cm^{-1}) in the case of NF_3, due mostly to the incorporation of higher levels of electron correlation within HEAT. There is also a large discrepancy in the scalar relativistic contributions to the total atomization energy as determined in the current study and those reported in Grant et al.;[21] 104 cm^{-1} for NF_3, 165 cm^{-1} for NF_3^+, and 116 cm^{-1} for NF_2^+. Attempts to reproduce the previous relativistic contributions were unsuccessful, defined as frozen-core CISD mass-velocity and one-electron Darwin (MVD) calculations with a cc-pVTZ basis. We attribute the inability to reproduce these results to a possible typo in

Table 2 of their article.

While at first glance the difference between previous theoretical and HEAT-calculated adiabatic ionization energies is marginal, the crux of this study lies in the improvement of the total atomization energies of NF_3, NF_3^+, and NF_2^+.

ATcT Results

The most recently publicly available version of ATcT results as of this writing (ATcT TN ver. 1.202)[42,76] reports the adiabatic ionization energy of NF_3, IE(NF_3) = 12.636 ± 0.023 eV, and the dissociative ionization threshold $AE_0(NF_2^+/NF_3)$ = 14.105 ± 0.007 eV (see Table 1). Clearly, the current HEAT values: IE(NF_3) = 12.647 ± 0.010 eV and $AE_0(NF_2^+/NF_3)$ = 14.112 ± 0.007 eV and the ATcT values are in very good agreement. The enthalpy of formation of NF_3 in this version is $\Delta_f H_0^\circ$ = -125.84 ± 0.55 kJ/mol (equivalent to -131.56 ± 0.55 kJ/mol at 298.15 K; cf. to -132.09 ± 1.13 kJ/mol in JANAF[81] or -131.7 ± 1.0 kJ/mol in Gurvich et al.[82]). The ATcT enthalpy of formation is equivalent to $TAE_0(NF_3)$ = 828.19 ± 0.54 kJ/mol, which is very nearly 3.0 kJ/mol higher than the CCSD(T)/CBS value of 825.22 kJ/mol,[21] but only 0.9 kJ/mol lower than the current HEAT result of 829.09 kJ/mol (Table 3).

One particular aspect is of relevance here: the ATcT results for IE(NF_3), $AE_0(NF_2^+/NF_3)$, and $TAE_0(NF_3)$ that are discussed above are entirely independent from the current HEAT calculations, but the rather close agreement between ATcT results and HEAT computations effectively tends to serve as mutual validation.

The variance decomposition analysis[83] indicates that the relevant contributors to the predicted adiabatic ionization energy of NF_3 in ver. 1.202 of ATcT TN are entirely from various mid-level computations: W1 value for IE(NF_3) (33.6%), CCSD(T)/CBS values for IE(NF_3) (17.8%) and $TAE_0(NF_3^+)$ (12.5%) from Grant et al.,[21] followed by the IE(NF_3) obtained at the G4 level (10.1%), CCSD(T)/CBS level by Ricca[20] (8.4%), as well as G3X(6.2%), CBS-APNO(5.9%), and CBS-QB3(5.5%) levels of theory. It should be mentioned here that at

the time of the introduction of NF_3 to the TN, the significantly higher values for IE(NF_3) inferred from experiments (see Table 1) were also initially included in the interim exploratory versions of ATcT TN, but were ultimately blocked (i.e. given zero weight) because the ATcT statistical analysis was suggesting that these are most likely outliers.

For $AE_0(NF_2^+/NF_3)$ the variance decomposition indicates that the primary contributor to the ATcT value in ver. 1.202 is the experimental onset of 14.100 ± 0.008 eV (62.3%). While not insignificant, the remaining contributions are at a much lower level: the experimental adiabatic ionization energy of NF_2 of 11.628 ± 0.011 eV (7.6%) determined by Berkowitz et al.,[14] the W1 value for $AE_0(NF_2^+/NF_3)$ of 14.124 ± 0.040 eV (2.5%), the experimental IE(NF_2) = 11.62 ± 0.02 eV determined by Cornford et al.[84] (2.3%), the computed $TAE_0(NF_2)$ at the FPD level of theory[85] (2.2%), the experimental $AE_0(NF_2^+/NF_2)$ = 12.514 ± 0.020 eV of Berkowitz et al.[14] (2.1%), followed by a number of smaller contributions (amounting to 1.6% or less each).

For the enthalpy of formation of NF_3 itself, the variance decomposition indicates that the top three contributors are from experiment: the calorimetric determination by Sinke of the hydrogenation of NF_3 producing aqueous HF[86] (24.9%), the related calorimetric determination of decomposition of NF_3 to N_2 and F_2 by Sinke[87] (18.5%), and the older calorimetric determination by Armstrong et al. of the hydrogenation of NF_3 producing aqueous HF[88] (13.1%). This is followed by the difference in total atomization energies of NF_3 and NH_3 at the FPD level of theory[85] (4.6%), the experimental $AE_0(NF_2^+/NF_3)$ determined by Berkowitz et al.[14] (3.7%), the $TAE_0(NF_2)$ (3.6%) and $TAE_0(NF_3)$ (3.3%), both at the FPD level of theory,[85] the experimental IE(NF_2) determined by Berkowitz et al.[14] (2.0%), and a number of even smaller contributions.

Since its publication, the version of ATcT TN discussed above was further expanded by additions of new chemical species, ultimately producing ATcT TN ver. 1.220. Of these expansions, the most significant is the addition of a number of key boron-containing species, the results of which are being reported elsewhere.[77] However, it should be mentioned that the

expansions occurring between ATcT TN ver. 1.202 and ver. 1.220 impacted minimally the thermochemistry related to NF_3: the resulting ATcT values for $IE(NF_3)$ and $AE_0(NF_2^+/NF_3)$ that were given above are the same, and the enthalpy of formation and total atomization energy of NF_3 have undergone insignificant changes, becoming $\Delta_f H_0^\circ(NF_3)$ = -125.90 ± 0.54 kJ/mol (equivalent to -131.61 ± 0.54 kJ/mol at 298.15 K) and $TAE_0(NF_3)$ = 828.28 ± 0.54 kJ/mol.

In order to make use of the new theoretical results for NF_3 for further improving the ATcT thermochemistry of NF_3, NF_3^+, and NF_2^+, the HEAT results were added to the thermochemical network, generating a new version of ATcT TN (ver. 1.222). The refurbished ATcT values are entirely compatible both with the earlier ATcT values and with the HEAT values, and the concomitant uncertainties are improved. As expected, the largest improvement is to the adiabatic ionization energy, which was in earlier versions dependent exclusively on mid-level computations (*vide supra*), shrinking its uncertainty by a factor of nearly 3 and becoming $IE(NF_3)$ = 12.644 ± 0.007 eV. The slight shift to higher values (by 0.008 eV) is comfortably contained within the previous uncertainty. The uncertainty of the dissociative ionization threshold, which was linked primarily to experimental data (*vide supra*), also improves, although the changes here are more modest, becoming $AE_0(NF_2^+/NF_3)$ = 14.108 ± 0.005 eV. The enthalpy of formation of NF_3, which in earlier versions relied heavily on calorimetry, becomes now $\Delta_f H_0^\circ(NF_3)$ = -126.27 ± 0.39 kJ/mol (equivalent to -131.99 ± 0.39 kJ/mol at 298.15 K), corresponding to $TAE_0(NF_3)$ = 828.66 ± 0.38 kJ/mol. The uncertainties of these values have somewhat improved, and the value for $TAE_0(NF_3)$ has slightly shifted (by 0.47 kJ/mol) toward the HEAT value, with the shift again entirely contained within the original uncertainty of ± 0.54 kJ/mol.

Evidently, the introduction of the highly accurate HEAT values into the TN makes the improved ATcT values dependent on them. In that sense, it is beneficial that these were independently mutually validated in the previous versions of ATcT TN, confirming that they are entirely consistent.

As expected, the introduction of the HEAT results has a noticeable impact on the provenances of the improved ATcT values. Thus, for IE(NF_3), now the primary contributors are the new theoretical results: the computed IE(NF_3) (43.3%) and $TAE_0(NF_3^+)$ (38.8%). Beyond these two, the contributions start fading rather rapidly, incorporating the HEAT value for $TAE_0(NF_3)$(3.1%), the IE(NF_3) from W1(2.7%), the calorimetric determination of Sinke of the hydrogenation of NF_3 producing aqueous HF[86](1.5%), the theoretical IE(NF_3) obtained by Grant et al.[21] (1.4%), the calorimetric determination of decomposition of NF_3 to N_2 and F_2 by Sinke[87] (1.1%), followed by even smaller (less than 1% each) contributors.

For $AE_0(NF_2^+/NF_3)$ the primary contributor remains the experimental dissociative photoionization threshold of Berkowitz et al.[14] (34.6%), followed by the newly introduced HEAT values for the same quantity (22.5%) and $TAE_0(NF_2^+)$(15.5%). As in the case of IE(NF_3), beyond these three, the contributions become noticeably smaller: experimental IE(NF_2) = 11.628 ± 0.011 of Berkowitz et al.[14] (3.6%), HEAT $TAE_0(NF_3)$ (3.4%), the mentioned calorimetric determination by Sinke of the hydrogenation of NF_3[86] (1.7%), W1 $AE_0(NF_2^+/NF_3)$ (1.4%), the mentioned calorimetric determination of decomposition of NF_3 to N_2 and F_2 by Sinke[87] (1.2%), experimental IE(NF_2) by Cornford et al.[84] (1.1%), followed by a number of smaller (1.0% or less) contributions.

Finally, for $\Delta_f H_0^\circ(NF_3)$ itself, the primary contributor becomes the HEAT $TAE_0(NF_3)$ (26.0%), followed by the experimental calorimetries of Sinke[86,87] (12.9% and 9.5%, respectively), HEAT $TAE_0(NF_2^+)$ (7.6%), the calorimetric determination of Armstrong et al.[88] (6.7%), the HEAT IE(NF_3) and $TAE_0(NF_3^+)$(4.9% and 4.5%, respectively), the experimental $AE_0(NF_2^+/NF_3)$ of Berkowitz et al.[14] (4.4%), HEAT $AE_0(NF_2^+/NF_3)$ (2.8%), the difference between $TAE_0(NF_3)$ and $TAE_0(NH_3)$ calculated at the FPD level of theory[85] (2.3%), and a sequence of other smaller contributors (at the level of 1.7% or less).

Interpretation of Experimental Features

With calculated ionization energy, dissociative ionization threshold, and the barrier to inversion for NF_3^+ in hand, we turn toward the previous interpretation of the partially vibrationally resolved photoelectron spectrum of NF_3 recorded by Berkowitz and Greene.[12] Figure 1 displays the raw experimental data in the upper panel, and the lower panel is the same data smoothed by a three-point average and normalized. The experimentally inferred ionization threshold is marked by vertical line A at 13.0 eV (black, dotted) in the lower panel, while line B (red, dashed) indicates the location of the HEAT-predicted ionization threshold (column 3 in Table 2). It is impossible to assert any definitive experimental ionization threshold in the vicinity of lines A and B due to the aforementioned unfavorable Franck-Condon factors associated with this transition. This issue is compounded by the fact that the experimental data begins roughly 0.12 eV higher than the theoretically-predicted threshold.

Line C (black, dotted) denotes the peak maximum of 13.75 eV along with the barrier to inversion of NF_3^+ as estimated in the literature.[12] This value was assigned based upon tentative observation of partial-vibrational resolution in the photoelectron spectrum; the hypothesis being that the closely-spaced peaks just beyond the maximum of the broad progression were in fact bifurcated vibrational intervals as referenced to the more widely-spaced peaks on the lower energy side of the maximum, where the higher-energy intervals were estimated as roughly half that of the lower energy region. This, combined with a qualitative estimate of the acceptable magnitude of such a barrier in NF_3^+ based upon *ab initio* calculations of barrier heights for PF_3 and PF_3^+ (Berkowitz and Greene[12] and references therein), yielded a barrier height for NF_3^+ to be roughly 0.75 eV, approximately the distance between the previously experimentally-estimated ionization threshold (13.0 eV) and the peak maximum (13.75 eV).

Line D (red, dashed), however, indicates the HEAT-calculated barrier to inversion at roughly 13.160 eV, the sum of the ionization threshold (12.647 eV) and barrier height, 0.513 eV. This assignment is nearly 0.6 eV lower in energy than the previous experimental barrier.

It is difficult to declare any distinct change in the vibrational interval near line D in a spirit similar to that done in previous work near line C, due to the experimental resolution, low signal-to-noise ratio, and lower overall intensity in this region of the spectrum. More important, however, is the stark difference between the calculated barrier to inversion and the hypothesized experimental assignment. This calls into question, first, the validity of the experimentally-estimated barrier to inversion and second, the origin of the hypothetical change (or rather, 'loss') in the vibrational interval on the higher-energy side of the peak maximum.

The experimental assignment, it should be mentioned, was acknowledged as only an estimation based upon intuitive arguments with available data at the time. As to the latter, possible explanations of loss of vibrational structure in photoelectron spectra include appearance thresholds of smaller molecular fragments or the presence of near-lying cation excited states.[19] A threshold photoelectron-photoion coincidence (tPEPICO) study performed by Seccombe et al.[11] reports the 50 % crossover threshold from NF_3^+ to NF_2^+ to occur at 14.10 ± 0.05 eV, which, generally speaking, is typically not far from AE_{298}, albeit it should be assigned a somewhat larger uncertainty and corrected by +0.059 eV to compensate for the internal energy of NF_3, leading to $AE_0(NF_2^+/NF_3)$ = 14.11 ± 0.08 eV. With the exception of the low onset reported by Rüede et al.,[18] other previous experimental data[13,14,78] report similar values for the appearance threshold (see Table 1). Of these, the most reliable and accurate seems to be the photoionization mass spectrometric onset by Berkowitz et al.,[14] reported as 883.0 ± 0.5 Å at 298 K, which, after correction for the internal energy of NF_3 becomes $AE_0(NF_2^+/NF_3)$ = 14.100 ± 0.008 eV. ATcT reports 14.105 ± 0.007 eV (*vide supra*). All of these are apparently confirmed by the HEAT-calculated value for $AE_0(NF_2^+/NF_3)$ = 14.112 ± 0.010 eV (see Table 1). The dissociative ionization onset is marked as line E in Figure 1, beyond which any discernible vibrational structure for NF_3^+ appears to be lost.

Seccombe et al.[11] also reported a 'first onset' of NF_2^+, significantly lower in energy than the 50% crossover threshold, at approximately 13.95 ± 0.05 eV. However, both in straightforward

photoionization mass spectrometry (PIMS) and in PEPICO, the 'first onset' is always red-shifted by the thermal tail that wanes exponentially toward lower energy caused by the thermally equilibrated internal energy of the NF_3 parent and thus does not correspond to a legitimate thermodynamic onset.[4] Indeed Seccombe et al.[11] attribute this threshold value only to instrumental sensitivity and not to thermodynamics, based on a similar argument presented by Asher and Ruscic[2] for a considerably lower value of the appearance threshold of CF_3^+ from CF_3Br. It would then be much more likely to see a change coincide with ATcT and HEAT-calculated estimates at line E. Again, however, the resolution and signal-to-noise prevent any unambiguous declaration of structure loss in this region of the spectrum.

The same threshold PEPICO study[11] reports ionization energies to several of the lowest-lying NF_3^+ electronic states, taken from the earlier work of Bassett and Lloyd.[17] Vertical excitation energies reported there, accompanied by calculations performed in the current work are located in Table 4. The $\tilde{X}^+$ state is associated with the ionization of an electron from the $4a_1$ lone pair orbital on the nitrogen atom. The next lowest-lying cation electronic states are the unresolved $\tilde{A}^+/\tilde{B}^+$ states, formed by ionization of a fluorine lone-pair electron. Previous studies[11,17,78] predict the $^2A_2$ state to lie higher in energy than the degenerate ^2E state from a combination of *ab initio* calculations and photoelectron spectroscopy, although the corresponding peaks were not resolvable experimentally. Here, EOM-CCSD(T)(a)* calculations reverse this ordering, with the $^2A_2$ state lying 0.36 eV lower in energy than the first ^2E state. Regardless of the relative ordering of these electronic states, previous experiments and high-level calculations agree in their prediction of the next lowest-lying electronic state to lie at minimum 2 eV above the calculated vertical ionization energy of $^2A_1$. While these energies should only be considered qualitatively, it is enough to reason that there is no sufficient interference of other electronic states with the initial ionization band that could explain any 'loss' in structure.

Based on these arguments, neither the fragmentation threshold nor nearby-lying cation excited states are responsible for the mysterious change (or loss) in vibrational structure

on the high-energy side of the photoelectron spectrum for the first ionization of NF_3. The low signal-to-noise ratio throughout the spectrum raises suspicion as to the existence of any vibrational structure beyond the peak maximum. The photoelectron spectrum reported by Seccombe et al.[11] is not sufficiently resolved to display any kind of vibrational structure similar to that shown in Figures 1 and 2, and we assert that any deliberate comparison or assignment of a loss in structure is impossible with the current experimental resolution (or signal-to-noise) of either study.

Franck-Condon Simulation

Figure 2 displays the experimental spectrum[12] smoothed by a three-point average (black), overlaid by a variational Franck-Condon simulation (red, see Computational Details section labeled 'Franck-Condon Simulations'). The peak maximum is chosen to align with the HEAT-calculated vertical ionization energy in Table 2, and no empirical scaling or influence is present in the simulation. The photoelectron spectrum of Berkowitz and Greene[12] appears to have a sloping background that grows toward higher energy. It is unclear if this is a spurious photoelectron background (which would not be entirely unusual in photoelectron spectroscopy), or if this perhaps corresponds to a superposition with the beginning of the Franck-Condon envelope of the next electronic state in NF_3^+. In our simulation, we correct for this apparent background by arbitrarily adding a simple linearly sloping background, as depicted in Figure 2.

The salient broad peak is well-reproduced in the simulation, with the most important comparison being the distance between the peak maximum and the ionization threshold, corresponding roughly to 1.06 eV. This is in excellent agreement with the HEAT-calculated difference between adiabatic and vertical ionization energies (1.07 eV). The HEAT-calculated ionization threshold is indicated by the vertical red dashed line in Figure 2.

As mentioned previously, we make no attempt to assign any possible vibrational peaks, instead choosing to keep the discussion purely qualitative in nature. Only symmetric modes

are included in the simulation, with resulting vibrational peaks dominated by combinations of the symmetric stretch (ν_1) and symmetric umbrella deformation (ν_2). This is not surprising due to the appreciable geometry change in both the N-F bond length and the bending angle upon ionization (calculated geometries may be found in the Supporting Information, Table 4). The FWHM used in the simulation to convolve the peaks is chosen arbitrarily to match experiment visually (0.045 eV, or 363 cm^{-1}), as the experimental resolution pertinent to the vibrational peaks (which include unresolved rotational substructure) is likely to be appreciably larger than the resolution obtained as FWHM for the atomic $^2P_{1/2}$ peak of Xe^+ (0.024 eV[12]).

Because the simulation emulates the HEAT-calculated difference between adiabatic and vertical ionization energies and visually reproduces the previous experiment quite well, it suffices to say that previous experimental estimates of the ionization threshold were plagued by unfavorable Franck-Condon factors near the origin, and the adiabatic onset for ionization of NF_3 is most likely inaccessible to experimental detection using conventional photoelectron spectroscopy or photoionization mass spectrometry. This results in vast overestimation of the experimental ionization energy, and we assert that the theoretically-predicted value is likely very close to the true threshold value.

Conclusions

High-accuracy *ab initio* thermochemical predictions for the ionization energy of NF_3, inversion barrier height of NF_3^+, and the dissociative photoionization threshold for $NF_2^+ + F$ from NF_3 instigates a discussion of previous experimental assignments of the first ionization band of NF_3. Based on the discrepancies that arise, updated assignments are interpreted and the loss in vibrational spacing on the high energy side of the experimental ionization band is discussed. The adiabatic ionization energy of NF_3 is calculated to be 12.647 $\pm$ 0.010 eV, while the vertical ionization energy is computed 1.073 eV higher, at 13.720 $\pm$ 0.01 eV. Rudi-

mentary anharmonic Franck-Condon simulations are included that qualitatively reproduce the broad spectral features observed in experiment. Higher-resolution experimental data is warranted to justify any additional effort to produce more detailed spectral simulations and beyond-speculative analysis of any vibrational structure, an endeavor that the authors intend to explore in a future publication.

Acknowledgement

We mourn the loss of our great mentor, colleague, and friend, John F. Stanton, who passed in the midst of the submission process of this manuscript. He will be greatly missed. The authors gratefully acknowledge John P. Greene (ANL) for his permission to reproduce in the current work the photoelectron spectrum of NF_3 recorded in a prior publication[12] using the archived spectral data. M.R.B. expresses sincere gratitude to Marie-Aline Martin-Drumel, Ugo Jacovella, and Bérenger Gans for their encouragement, advice, and helpful discussion throughout the preparation of this manuscript. The work at Argonne National Laboratory (D.H.B. and B.R.) was supported by the U.S. Department of Energy, Office of Science, Office of Basic Energy Sciences, Division of Chemical Sciences, Geosciences and Biosciences, under Contract No. DE-AC02-06CH11357, through the Gas-Phase Chemical Physics Program. The work at University of Florida (M.R.B., P.R.F., K.E.W., and J.F.S.) was supported by the U.S. Department of Energy, Office of Basic Energy Sciences under Award DESC0018164. The work by M.R.B. was also supported by the Chateaubriand Fellowship of the Office for Science and Technology of the Embassy of France in the United States. Most of the authors (M.R.B., P.R.F., D.H.B., B.R., J.F.S.) are members of the ATcT Task Force One. The Active Thermochemical Tables are a U.S. Department of Energy Office of Science Public Reusable Research (DOE SC PuRe) Data Resource[89]

Supporting Information Available

Molecular equilibrium geometries for all compounds, fundamental frequencies of NF_3, NF_3^+, atomic and molecular electronic energy contributions to total atomization energies for all compounds.

References

(1) Horn, M.; Oswald, M.; Oswald, R.; Botschwina, P. Calculated vibrational structure of the photoelectron spectra of free radicals. *Berichte der Bunsengesellschaft für Physikalische Chemie* **1995**, *99*, 323–331.

(2) Asher, R. L.; Ruscic, B. On the heats of formation of trifluoromethyl radical CF_3 and its cation CF_3^+. *The Journal of Chemical Physics* **1997**, *106*, 210–221.

(3) Botschwina, P.; Horn, M.; Oswald, R.; Schmatz, S. Theoretical investigations of free radicals and negative molecular ions and their calculated photoelectron spectra. *Journal of Electron Spectroscopy and Related Phenomena* **2000**, *108*, 109–122.

(4) Ruscic, B. Photoionization mass spectroscopic studies of free radicals in gas phase: why and how. *Research Advances in Physical Chemistry* **2000**, *1*, 39–75.

(5) Bowman, J. M.; Huang, X.; Harding, L. B.; Carter, S. The determination of molecular properties from MULTIMODE with an application to the calculation of Franck-Condon factors for photoionization of CF_3 to CF_3^+. *Molecular Physics* **2006**, *104*, 33–45.

(6) Dossmann (Soldi-Lose), H.; Garcia, G. A.; Nahon, L.; De Miranda, B. K. C.; Alcaraz, C. Comprehensive vacuum ultraviolet photoionization study of the CF_3 trifluoromethyl radical using synchrotron radiation. *The Journal of Chemical Physics* **2012**, *136*, 204304/1–204304/8.

(7) Ruscic, B.; Pinzon, R. E.; Morton, M. L.; von Laszevski, G.; Bittner, S. J.; Nijsure, S. G.; Amin, K. A.; Minkoff, M.; Wagner, A. F. Introduction to Active Thermochemical Tables: Several "key" enthalpies of formation revisited. *The Journal of Physical Chemistry A* **2004**, *108*, 9979–9997.

(8) Ruscic, B.; Pinzon, R. E.; von Laszevski, G.; Kodeboyina, D.; Burcat, A.; Leahy, D.; Montoya, D.; Wagner, A. F. Active Thermochemical Tables: thermochemistry for the 21st century. *Journal of Physics: Conference Series* **2005**, *16*, 561–570.

(9) Prather, M. J.; Hsu, J. NF_3, the Greenhouse Gas Missing from Kyoto. *Geophysical Research Letters* **2008**, *35*, L12810/1–L12810/3.

(10) Prather, M. J.; Hsu, J. Correction to "NF_3, the Greenhouse Gas Missing from Kyoto". *Geophysical Research Letters* **2010**, *37*, L11807.

(11) Seccombe, D. P.; Jarvis, G. K.; Fisher, B. O.; Tuckett, R. P. Fragmentation of the valence electronic states of NF_3^+ studied by threshold photoelectron–photoion coincidence spectroscopy. *Chemical Physics* **1999**, *250*, 335–346.

(12) Berkowitz, J.; Greene, J. P. The barrier to inversion in NF_3^+. *The Journal of Chemical Physics* **1984**, *81*, 3383–3386.

(13) Dibeler, V. H.; Walker, J. A. Mass spectrometric study of photoionization. XIV. Nitrogen trifluoride and trifluoramine oxide. *Inorganic Chemistry* **1969**, *8*, 1728–1733.

(14) Berkowitz, J.; Greene, J. P.; Foropoulos, J.; Nesković, O. M. Bonding and ionization energies of N–F and P–F compounds. *The Journal of Chemical Physics* **1984**, *81*, 6166–6175.

(15) Potts, A. W.; Lempka, H. J.; Streets, D. G.; Price, W. C. Photoelectron spectra of the halides of elements in groups III, IV, V and VI. *Philosophical Transactions of the Royal Society of London. Series A, Mathematical and Physical Sciences* **1970**, *268*, 59–76.

(16) Potts, A. W.; Price, W. C. Photoelectron spectra and valence shell orbital structures of groups V and VI hydrides. *Proceedings of the Royal Society of London. A. Mathematical and Physical Sciences* **1972**, *326*, 181–197.

(17) Bassett, P. J.; Lloyd, D. R. Photoelectron spectra of halides. Part III. Triflourides and oxide trifluorides of nitrogen and phosphorus, and phosphorus oxide trichloride. *Journal of the Chemical Society, Dalton Transactions* **1972**, 248–254.

(18) Rüede, R.; Troxler, H.; Beglinger, C.; Jungen, M. The dissociation energies of the positive ions NH_3^+, NF_3^+, PH_3^+, PF_3^+, and PCl_3^+. *Chemical Physics Letters* **1993**, *203*, 477–481.

(19) Baumgärtel, H.; Jochims, H.-W.; Rühl, E.; Bock, H.; Dammel, R.; Minkwitz, J.; Nass, R. Photoelectron spectra and molecular properties. 112. Photoelectron and photoionization mass spectra of the fluoroamines $NH_{3-n}F_n$. *Inorganic Chemistry* **1989**, *28*, 943–949.

(20) Ricca, A. Heats of formation for NF_n (n=1-3) and NF_n^+ (n=1-3). *Chemical Physics Letters* **1998**, *294*, 454–458.

(21) Grant, D. J.; Wang, T.-H.; Vasiliu, M.; Dixon, D. A.; Christe, K. O. F^+ and F^- affinities of simple N_xF_y and O_xF_y compounds. *Inorganic Chemistry* **2011**, *50*, 1914–1925.

(22) Raghavachari, K.; Trucks, G. W.; Pople, J. A.; Head-Gordon, M. A fifth-order perturbation comparison of electron correlation theories. *Chemical Physics Letters* **1989**, *157*, 479–483.

(23) Bartlett, R. J.; Watts, J. D.; Kucharski, S. A.; Noga, J. Non-iterative fifth-order triple and quadruple excitation energy corrections in correlated methods. *Chemical Physics Letters* **1990**, *165*, 513–522.

(24) Stanton, J. F. Why CCSD(T) works: a different perspective. *Chemical Physics Letters* **1997**, *281*, 130–134.

(25) Ruscic, B.; Bross, D. H. *Computer Aided Chemical Engineering*; Elsevier, 2019; Vol. 45; pp 3–114.

(26) Tajti, A.; Szalay, P. G.; Császár, A. G.; Kállay, M.; Gauss, J.; Valeev, E. F.; Flowers, B. A.; Vázquez, J.; Stanton, J. F. Heat: High accuracy extrapolated *ab initio* thermochemistry. *The Journal of Chemical Physics* **2004**, *121*, 11599–11613.

(27) Bomble, Y. J.; Vázquez, J.; Kállay, M.; Michauk, C.; Szalay, P. G.; Császár, A. G.; Gauss, J.; Stanton, J. F. High-accuracy extrapolated *ab Initio* thermochemistry. II. Minor improvements to the protocol and a vital simplification. *The Journal of Chemical Physics* **2006**, *125*, 064108/1–064108/8.

(28) Harding, M. E.; Vázquez, J.; Ruscic, B.; Wilson, A. K.; Gauss, J.; Stanton, J. F. High-accuracy extrapolated *ab initio* thermochemistry. III. Additional improvements and overview. *The Journal of Chemical Physics* **2008**, *128*, 114111/1–114111/15.

(29) Thorpe, J. H.; Lopez, C. A.; Nguyen, T. L.; Baraban, J. H.; Bross, D. H.; Ruscic, B.; Stanton, J. F. High-accuracy extrapolated *ab initio* thermochemistry. IV. A modified recipe for computational efficiency. *The Journal of Chemical Physics* **2019**, *150*, 224102/1–224102/16.

(30) Thorpe, J. H.; Kilburn, J. L.; Feller, D.; Changala, P. B.; Bross, D. H.; Ruscic, B.; Stanton, J. F. Elaborated thermochemical treatment of HF, CO, N_2, and H_2O: Insight into HEAT and its extensions. *The Journal of Chemical Physics* **2021**, *155*, 184109/1–184109/13.

(31) Thorpe, J. H.; Feller, D.; Bross, D. H.; Ruscic, B.; Stanton, J. F. Sub 20 cm^{-1} computational prediction of the CH bond energy – a case of systematic error in computational thermochemistry. *Physical Chemistry Chemical Physics* **2023**, *25*, 21162–21172.

(32) Martin, J. M. L.; De Oliveira, G. Towards standard methods for benchmark quality *ab initio* thermochemistry—W1 and W2 theory. *The Journal of Chemical Physics* **1999**, *111*, 1843–1856.

(33) Boese, A. D.; Oren, M.; Atasoylu, O.; Martin, J. M. L.; Kállay, M.; Gauss, J. W3 theory: Robust computational thermochemistry in the kJ/mol accuracy range. *The Journal of Chemical Physics* **2004**, *120*, 4129–4141.

(34) Karton, A.; Rabinovich, E.; Martin, J. M. L.; Ruscic, B. W4 theory for computational thermochemistry: In pursuit of confident sub-kJ/mol predictions. *The Journal of Chemical Physics* **2006**, *125*, 144108/1–144108/17.

(35) Karton, A.; Martin, J. M. L. Explicitly correlated W_n theory: W1-F12 and W2-F12. *The Journal of Chemical Physics* **2012**, *136*, 124114/1–124114/12.

(36) Sylvetsky, N.; Peterson, K. A.; Karton, A.; Martin, J. M. L. Toward a W4-F12 approach: Can explicitly correlated and orbital-based *ab initio* CCSD(T) limits be reconciled? *The Journal of Chemical Physics* **2016**, *144*, 214101/1–214101/13.

(37) Klippenstein, S. J.; Harding, L. B.; Ruscic, B. Ab initio computations and Active Thermochemical Tables hand in hand: Heats of formation of core combustion species. *The Journal of Physical Chemistry A* **2017**, *121*, 6580–6602.

(38) East, A. L. L.; Allen, W. D. The heat of formation of NCO. *The Journal of Chemical Physics* **1993**, *99*, 4638–4650.

(39) Császár, A. G.; Allen, W. D.; Schaefer, H. F. In pursuit of the *ab initio* limit for conformational energy prototypes. *The Journal of Chemical Physics* **1998**, *108*, 9751–9764.

(40) Schuurman, M. S.; Muir, S. R.; Allen, W. D.; Schaefer, H. F. Toward subchemical accuracy in computational thermochemistry: Focal point analysis of the heat of for-

mation of NCO and [H,N,C,O] isomers. *The Journal of Chemical Physics* **2004**, *120*, 11586–11599.

(41) Peterson, K. A.; Feller, D.; Dixon, D. A. Chemical accuracy in ab initio thermochemistry and spectroscopy: current strategies and future challenges. *Theoretical Chemistry Accounts* **2012**, *131*, 1079/1–1079/20.

(42) Ruscic, B.; Bross, D. H. 2024; Active Thermochemical Tables (ATcT) values based on ver. 1.202 of the Thermochemical Network, Argonne National Laboratory: Lemont, IL, doi: 10.17038/CSE/2440256, available at ATcT.anl.gov.

(43) Curtiss, L. A.; Redfern, P. C.; Raghavachari, K.; Pople, J. A. Gaussian-3X (G3X) theory: Use of improved geometries, zero-point energies, and Hartree–Fock basis sets. *The Journal of Chemical Physics* **2001**, *114*, 108–117.

(44) Curtiss, L. A.; Redfern, P. C.; Raghavachari, K. Gaussian-4 theory. *The Journal of Chemical Physics* **2007**, *126*, 084108/1–084108/12.

(45) Ochterski, J. W.; Petersson, G. A.; Montgomery, J. A. A complete basis set model chemistry. V. Extensions to six or more heavy atoms. *The Journal of Chemical Physics* **1996**, *104*, 2598–2619.

(46) Montgomery, J. A.; Frisch, M. J.; Ochterski, J. W.; Petersson, G. A. A complete basis set model chemistry. VII. Use of the minimum population localization method. *The Journal of Chemical Physics* **2000**, *112*, 6532–6542.

(47) Simmie, J. M.; Somers, K. P. Benchmarking compound methods (CBS-QB3, CBS-APNO, G3, G4, W1BD) against the Active Thermochemical Tables: A litmus test for cost-effective molecular formation enthalpies. *The Journal of Physical Chemistry A* **2015**, *119*, 7235–7246.

(48) Noga, J.; Bartlett, R. J. The full CCSDT model for molecular electronic structure. *The Journal of Chemical Physics* **1987**, *86*, 7041–7050.

(49) Noga, J.; Bartlett, R. J. Erratum: The full CCSDT model for molecular electronic structure. *The Journal of Chemical Physics* **1988**, *89*, 3401–3401.

(50) Scuseria, G. E.; Schaefer, H. F. A new implementation of the full CCSDT model for molecular electronic structure. *Chemical Physics Letters* **1988**, *152*, 382–386.

(51) Kucharski, S. A.; Bartlett, R. J. An efficient way to include connected quadruple contributions into the coupled cluster method. *The Journal of Chemical Physics* **1998**, *108*, 9221–9226.

(52) Bomble, Y. J.; Stanton, J. F.; Kállay, M.; Gauss, J. Coupled-cluster methods including noniterative corrections for quadruple excitations. *The Journal of Chemical Physics* **2005**, *123*, 054101/1–054101/8.

(53) Crawford, T. D.; Stanton, J. F. Investigation of an asymmetric triple-excitation correction for coupled-cluster energies. *International Journal of Quantum Chemistry* **1998**, *70*, 601–611.

(54) Kállay, M.; Gauss, J. Approximate treatment of higher excitations in coupled-cluster theory. *The Journal of Chemical Physics* **2005**, *123*, 214105/1–21405/13.

(55) Kállay, M.; Gauss, J. Approximate treatment of higher excitations in coupled-cluster theory. II. Extension to general single-determinant reference functions and improved approaches for the canonical Hartree–Fock case. *The Journal of Chemical Physics* **2008**, *129*, 144101/1–144101/9.

(56) Oliphant, N.; Adamowicz, L. Coupled-cluster method truncated at quadruples. *The Journal of Chemical Physics* **1991**, *95*, 6645–6651.

(57) Kucharski, S. A.; Bartlett, R. J. The coupled-cluster single, double, triple, and quadruple excitation method. *The Journal of Chemical Physics* **1992**, *97*, 4282–4288.

(58) Kucharski, S. A.; Bartlett, R. J. Connected quadruples for the frequencies of O_3. *The Journal of Chemical Physics* **1999**, *110*, 8233–8235.

(59) Dunning, T. H. Gaussian basis sets for use in correlated molecular calculations. I. The atoms boron through neon and hydrogen. *The Journal of Chemical Physics* **1989**, *90*, 1007–1023.

(60) Kendall, R. A.; Dunning, T. H.; Harrison, R. J. Electron affinities of the first-row atoms revisited. Systematic basis sets and wave functions. *The Journal of Chemical Physics* **1992**, *96*, 6796–6806.

(61) Spiegel, M.; Semidalas, E.; Martin, J. M. L.; Bentley, M. R.; Stanton, J. F. Post-CCSD(T) corrections to bond distances and vibrational frequencies: The power of Λ. *Molecular Physics* **2023**, *122*, e2252114/1–e2252114/12.

(62) Franke, P. R.; Stanton, J. F. Rotamers of methanediol: Composite *ab initio* predictions of structures, frequencies, and rovibrational constants. *The Journal of Physical Chemistry A* **2023**, *127*, 924–937.

(63) Matthews, D. A.; Cheng, L.; Harding, M. E.; Lipparini, F.; Stopkowicz, S.; Jagau, T.-C.; Szalay, P. G.; Gauss, J.; Stanton, J. F. Coupled-cluster techniques for computational chemistry: The CFOUR program package. *The Journal of Chemical Physics* **2020**, *152*, 214108/1–214108/35.

(64) Matthews, D. A.; Stanton, J. F. Non-orthogonal spin-adaptation of coupled cluster methods: A new implementation of methods including quadruple excitations. *The Journal of Chemical Physics* **2015**, *142*, 064108/1–064108/16.

(65) Matthews, D. A.; Stanton, J. F. Accelerating the convergence of higher-order coupled cluster methods. *The Journal of Chemical Physics* **2015**, *143*, 204103/1–204103/9.

(66) Matthews, D. A. Accelerating the convergence of higher-order coupled-cluster methods II: coupled-cluster Λ equations and dynamic damping. *Molecular Physics* **2020**, *118*, e1757774/1–e1757774/13.

(67) Stanton, J. F. and Gauss, J. and Cheng, L. and Harding, M. E. and Matthews, D. A. and Szalay, P. G. CFOUR, a quantum chemical program package. `http://www.cfour.de.`

(68) Kállay, M. et al. The MRCC program system: Accurate quantum chemistry from water to proteins. *The Journal of Chemical Physics* **2020**, *152*, 074107/1–074107/18.

(69) Stanton, J. F. On the vibronic level structure in the NO_3 radical: II. Adiabatic calculation of the infrared spectrum. *Molecular Physics* **2009**, *107*, 1059–1075.

(70) Lanczos, C. An iteration method for the solution of the eigenvalue problem of linear differential and integral operators. *Journal of Research of the National Bureau of Standards* **1950**, *45*, 255–282.

(71) Stanton, J. F.; Bartlett, R. J. The equation of motion coupled-cluster method. A systematic biorthogonal approach to molecular excitation energies, transition probabilities, and excited state properties. *The Journal of Chemical Physics* **1993**, *98*, 7029–7039.

(72) Matthews, D. A.; Stanton, J. F. A new approach to approximate equation-of-motion coupled cluster with triple excitations. *The Journal of Chemical Physics* **2016**, *145*, 124102/1–124102/14.

(73) Feller, D.; Bross, D. H.; Ruscic, B. Enthalpy of formation of N2H4 (hydrazine) revisited. *The Journal of Physical Chemistry A* **2017**, *121*, 6187–6198.

(74) Changala, P. B.; Nguyen, T. L.; Baraban, J. H.; Ellison, G. B.; Stanton, J. F.;

Bross, D. H.; Ruscic, B. Active Thermochemical Tables: The adiabatic ionization energy of hydrogen peroxide. *The Journal of Physical Chemistry A* **2017**, *121*, 8799–8806.

(75) Feller, D.; Bross, D. H.; Ruscic, B. Enthalpy of formation of $C_2H_2O_4$ (oxalic acid) from high-level calculations and the Active Thermochemical Tables approach. *The Journal of Physical Chemistry A* **2019**, *123*, 3481–3496.

(76) Ruscic, B.; Bross, D. H. Accurate and reliable thermochemistry by data analysis of complex thermochemical networks using Active Thermochemical Tables: The case of glycine thermochemistry. *Faraday Discussions* **2025**, *256*, 345–372.

(77) Ruscic, B.; Bross, D. H. Active Thermochemical Tables: Should the enthalpy of formation of gas phase boron atom be revised? *Chemical Physics Letters* **2025**, *862*, 141841/1–141841/4.

(78) Mansell, P. I.; Danby, C. J.; Powis, I. Dissociation of state-selected nitrogen trifluoride cations. *Journal of the Chemical Society, Faraday Transactions 2* **1981**, *77*, 1449–1459.

(79) Feller, D. Application of systematic sequences of wave functions to the water dimer. *The Journal of Chemical Physics* **1992**, *96*, 6104–6114.

(80) Helgaker, T.; Klopper, W.; Koch, H.; Noga, J. Basis-set convergence of correlated calculations on water. *The Journal of Chemical Physics* **1997**, *106*, 9639–9646.

(81) M. W. Chase Jr., E. NIST-JANAF Thermochemical Tables. 4th edition, Journal of Physical and Chemical Reference Data, Monograph 9, doi: 10.18434/T42S31, 1998.

(82) Gurvich, L.; Veyts, I.; Alcock, C. *Thermodynamic Properties of Individual Substances*, 4th ed.; Parts 1 and 2; Hemisphere: New York, 1989; Vol. 1.

(83) Ruscic, B.; Feller, D.; Peterson, K. A. Active Thermochemical Tables: dissociation energies of several homonuclear first-row diatomics and related thermochemical values. *Theoretical Chemistry Accounts* **2014**, *133*, 1415/1–1415/12.

(84) Cornford, A. B.; Frost, D. C.; Herring, F. G.; McDowell, C. A. Ionization potentials of the difluoroamino radical by photoelectron spectroscopy and INDO calculations. *The Journal of Chemical Physics* **1971**, *54*, 1872–1873.

(85) Feller, D.; Peterson, K. A.; Dixon, D. A. A survey of factors contributing to accurate theoretical predictions of atomization energies and molecular structures. *The Journal of Chemical Physics* **2008**, *129*, 204105/1–204105/32.

(86) Sinke, G. C. Heat of reaction of hydrogen and nitrogen trifluoride. *Journal of Chemical and Engineering Data* **1965**, *10*, 295–296.

(87) Sinke, G. C. Enthalpy of dissociation of nitrogen trifluoride. *The Journal of Physical Chemistry* **1967**, *71*, 359–360.

(88) Armstrong, G. T.; Marantz, S.; Coyle, C. F. Heat of formation of nitrogen fluoride and the N-F bond energy. *Journal of the American Chemical Society* **1959**, *81*, 3798–3798.

(89) U.S. Department of Energy, Office of Science PuRe Data Resources at a glance. 2023; `https://science.osti.gov/Initiatives/PuRe-Data/Resources-at-a-Glance`, accessed December 2024.

TOC Graphic